Resolving the characteristics of morphotropic phase boundary in the $(1-x)Pb(Fe_{1/2}Nb_{1/2})O_3 - xPbTiO_3$ system: A combined dielectric and synchrotron x-ray diffraction study

Cite as: Appl. Phys. Lett. **93**, 182910 (2008); https://doi.org/10.1063/1.3012378
Submitted: 11 July 2008 . Accepted: 11 October 2008 . Published Online: 07 November 2008

Satendra Pal Singh, Dhananjai Pandey, Songhak Yoon, et al.

Resolving the characteristics of morphotropic phase boundary in the $(1-x)Pb(Fe_{1/2}Nb_{1/2})O_3-xPbTiO_3$ system: A combined dielectric and synchrotron x-ray diffraction study

Satendra Pal Singh,[1] Dhananjai Pandey,[1,a)] Songhak Yoon,[2] Sunggi Baik,[2] and Namsoo Shin[3]
[1]*School of Materials Science and Technology, Institute of Technology, Banaras Hindu University, Varanasi 221 005, India*
[2]*Department of Materials Science and Engineering, Pohang University of Science and Technology, Pohang 790-784, Republic of Korea*
[3]*Pohang Accelerator Laboratory, Pohang University of Science and Technology, Pohang 790-784, Republic of Korea*

(Received 11 July 2008; accepted 11 October 2008; published online 7 November 2008)

Frequency dependent dielectric studies on the mixed system $(1-x)Pb(Fe_{1/2}Nb_{1/2})O_3-xPbTiO_3$ reveal contributions from the electrodes, grain boundaries, and grains. It is shown that the intrinsic value of the dielectric permittivity coming only from the grains peaks at $x=0.08$. Analysis of synchrotron x-ray diffraction profiles using the Rietveld technique shows that this peaking is linked with a monoclinic to tetragonal morphotropic phase transition in the multiferroic system. © *2008 American Institute of Physics*. [DOI: 10.1063/1.3012378]

The last few years have witnessed revival of interest in the study of structure-property correlations in solid solutions of $PbTiO_3$ (PT) with other ferroelectric/antiferroelectric/relaxor ferroelectric oxide perovskites exhibiting a morphotropic phase boundary (MPB) in their phase diagrams. The impetus for this has come from the recent discovery of several monoclinic phases in the *Cm*,[1,2] *Cc*,[3,4] and *Pm* (Refs. 2, 5, and 6) space groups in the well known MPB systems such as $Pb(Zr_xTi_{1-x})O_3$ (PZT), $(1-x)[Pb(Mg_{1/3}Nb_{2/3})O_3]-xPbTiO_3$ (PMN–*x*PT), $(1-x)[Pb(Zn_{1/3}Nb_{2/3})O_3]-xPbTiO_3$ (PZN–*x*PT), and $(1-x)[Pb(Sc_{1/2}Nb_{1/2})O_3]-xPbTiO_3$. MPB has also been reported in the solid solutions of PT with multiferroic compounds such as $Pb(Fe_{1/2}Nb_{1/2})O_3$ (PFN) (Refs. 7 and 8) and $BiFeO_3$ (BF).[9] One of the characteristics of the MPB ceramics in the strongly insulating systems such as PZT and PMN–*x*PT is the peaking of dielectric permittivity (ε') for the MPB composition in the ε' versus composition (x) plots. Such a peaking of the ε' is not observed in the MPB systems containing multiferroic components such as $(1-x)Pb(Fe_{1/2}Nb_{1/2})O_3-xPbTiO_3$ (PFN–*x*PT) and $BiFeO_3-xPbTiO_3$ (BF–*x*PT). There is no satisfactory explanation for this at present. We show here that the interfacial (space charge) contributions, coming from grain boundaries and grain-electrode interfaces, to the overall measured value of the dielectric permittivity are responsible for masking the peaking of the ε' in the ε' versus x plots. Further, we show that the peak in the ε' versus x plot characteristic of a MPB system comes out unambiguously using high frequency data. In the highly insulating MPB systems such as PZT, this peaking of the dielectric permittivity has been linked to a tetragonal to monoclinic morphotropic phase transition.[1,4] However, for capturing the signatures of the monoclinic phases, one requires high resolution powder synchrotron x-ray diffraction data, as was done in the case of PZT.[10] No such high resolution synchrotron x-ray diffraction study has been carried out on the PFN–*x*PT system so far. We complement our dielectric studies with the results of Rietveld analysis of the powder synchrotron x-ray diffraction data which provide unambiguous evidence for the tetragonal to monoclinic phase transition in PFN–*x*PT across the MPB at $x=0.08$.

Pyrochlore phase free PFN–*x*PT ceramics were synthesized using wolframite precursor method.[11] The density of the samples was greater than 97% of the theoretical density. Synchrotron powder x-ray diffraction data were collected at 8C2 HRPD beamline at Pohang Light Source (PLS) in the 2θ range of $20°-130°$ at a step of 0.01°. The dielectric/impedance measurements were carried out using a Novocontrol Alpha-ATB high performance frequency analyzer. Rietveld refinements were carried out using the FULLPROF package.[12] In the refinements, pseudo-Voigt function and linear interpolation between the set background points with refinable height were used to define the profile shape and the background, respectively. It was found necessary to use anisotropic peak broadening in the refinements. The isotropic thermal parameter for Pb was found to be considerably large (~2.5), indicating Pb-site disorder, as reported by earlier

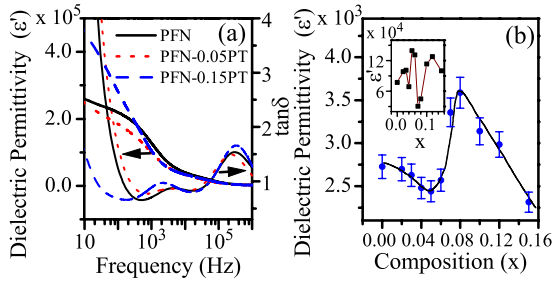

FIG. 1. (Color online) The variations in (a) the real part of the dielectric permittivity (ε') and loss tangent (tan δ) with frequency of PFN–*x*PT for $x=0.00$, 0.05, and 0.15, and (b) dielectric permittivity (ε') with composition (x) at 700 kHz. The inset of (b) shows the random variation in ε' with x at 1 kHz.

a)Author to whom correspondence should be addressed. Electronic mail: dpandey_bhu@yahoo.co.in.

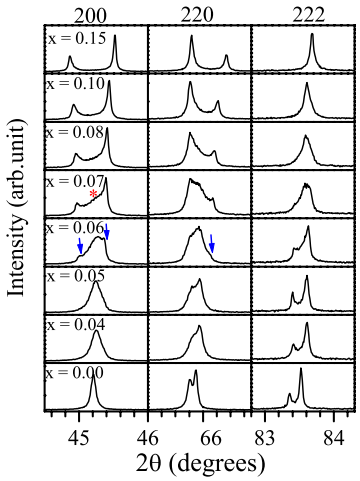

FIG. 2. (Color online) Evolution of the profiles of the 200, 220, and 222 pseudocubic reflections for PFN–xPT ($0.0 \leq x \leq 0.15$). A few tetragonal peaks and a monoclinic peak are marked with arrows and an asterisk for $x=0.06$ and 0.07, respectively.

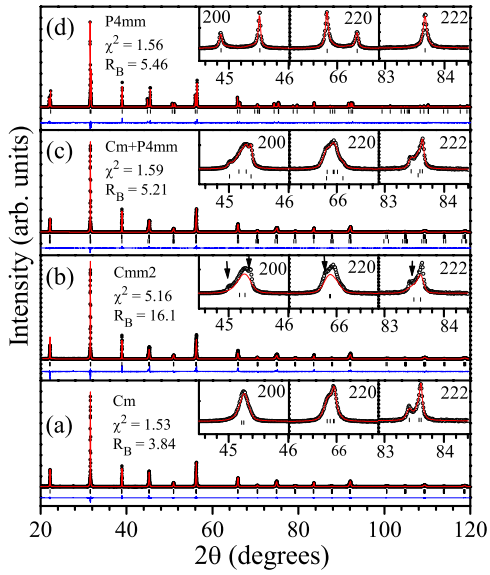

FIG. 3. (Color online) The observed (dots), calculated (continuous line), and difference (bottom line) profiles obtained after full pattern refinements using (a) monoclinic *Cm* space group for $x=0.04$, (b) orthorhombic *Cmm*2 space group for $x=0.06$, (c) coexistence of monoclinic (*Cm*) and tetragonal (*P*4*mm*) structures for $x=0.06$, and (d) tetragonal *P*4*mm* space group with very small fraction of coexisting monoclinic phase for $x=0.15$. Insets of the figure illustrate the quality of Rietveld fits for three selected (200, 220, and 222) pseudocubic reflections.

workers also.[13] Accordingly anisotropic thermal parameters were used for Pb, which resulted in lower χ^2 values.

Figure 1(a) shows the variation in the real part of the dielectric permittivity (ε') and tan δ with frequency for three typical compositions of PFN–xPT with $x=0.00$, $x=0.05$, and $x=0.15$. It is evident from this figure that the value of dielectric permittivity is very high ($\sim 2\times 10^5$) at lower frequencies but decreases with increasing frequency before stabilizing to values which are two orders of magnitude lower. The nearly linear variation in tan δ with frequency shown in Fig. 1(a) in the low frequency regime is usually attributed to the contribution from charge injected from the electrodes. On the other hand the other two peaks in the high frequency regime arise due to the contributions from the grain boundaries and grains, due to the difference in the relaxation times between the grain and grain boundary polarization processes.[14] The dipolar relaxation time in the grains is generally lower than that in the grain boundaries. Hence the contribution of grains will lead to a peak in tan δ at higher frequencies than those due to the grain boundaries.[14] The value of the dielectric permittivity becomes nearly frequency independent at frequencies above 400 kHz. The dielectric permittivity measured above this frequency will therefore be representative of the dielectric permittivity of grains only and hence the intrinsic value of the dielectric permittivity of the material also. The variation in intrinsic dielectric permittivity (ε') measured at 700 kHz with composition (x) shows a peak at $x=0.08$ [see Fig. 1(b)]. On the other hand the variation in ε' with x measured at 1 kHz, a frequency at which all the three polarization processes contribute, does not exhibit any systematic dependence on composition [see inset of Fig. 1(b)]. Such an anomalous peaking of the dielectric permittivity as a function of composition has been linked to a morphotropic phase transition in the technologically important PZT, PMN–xPT, and PZN–xPT.[8] We shall now proceed to show that the peak in the dielectric permittivity shown in Fig. 1(b) is indeed linked to a monoclinic to tetragonal morphotropic phase transition in PFN–xPT as a function of composition.

Figure 2 depicts the diffraction profiles of three representative pseudocubic reflections (200, 220, and 222) in the composition range of $0 \leq x \leq 0.15$. It is evident from this figure that for $x<0.05$, the 200 is a singlet, while 222 is a doublet, suggesting a rhombohedral structure. However, the 200 peak is much broader than either of the two 222 peaks. This anomalous broadening increases drastically with increasing PT content (x) for $x<0.05$, but disappears for $x \geq 0.08$. This suggests that the 200 peak for $x<0.05$ may not be a singlet. We have recently shown that such an anomalous broadening in PFN ($x=0$) is due to the monoclinic distortion of the lattice on a short range scale.[15] For $x>0.08$, the doublet nature of 200 and the singlet nature of 222 peaks suggest that the dominant phase is now tetragonal. For the intermediate compositions ($0.05 \leq x \leq 0.08$), the peak corresponding to both phases are clearly seen in Fig. 2. Using laboratory powder x-ray diffraction data, it was earlier[16] reported that for $x=0.06$ the structure is pure monoclinic in the *Cm* space group. But high resolution synchrotron x-ray powder diffraction data on the same sample shown in Fig. 2 clearly reveals a coexistence of the tetragonal and monoclinic phases.

In order to confirm the qualitative observations in the previous paragraph, we carried out Rietveld refinements using the FULLPROF package.[12] Figures 3(a), 3(c), and 3(d) depict the Rietveld fits in the 2θ range of $20°-120°$ for three

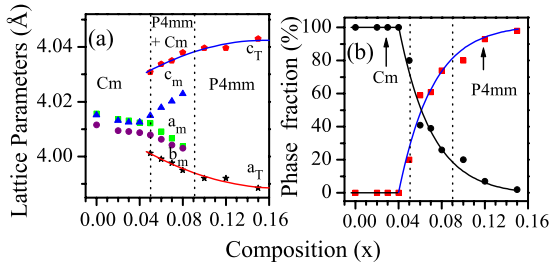

FIG. 4. (Color online) Composition dependent variations in (a) lattice parameters and (b) phase fractions of tetragonal and monoclinic phases.

TABLE I. Refined structural parameters of PFN–xPT for monoclinic structure in the Cm space group for $x=0.04$ and for tetragonal structure in the $P4mm$ space group for $x=0.15$.

	$a_m=5.6744(1)$ Å, $b_m=5.66925(6)$ Å, $c_m=4.0138(1)$ Å, and $\beta=90.114(9)$ (degrees) for $x=0.04$				$a=b=3.988\ 71(1)$ Å and $c=4.043\ 33(2)$ Å for $x=0.15$			
Ion	x	y	z	B (Å^2)	x	y	z	B (Å^2)
Pb^{+2}	0.0000	0.0000	0.0000	$\beta_{11}=0.017(2)$ $\beta_{22}=0.023(1)$ $\beta_{33}=0.029(2)$ $\beta_{13}=0.006(1)$	0.0000	0.0000	0.0000	$\beta_{11}=0.0350(4)$ $\beta_{22}=0.0350(4)$ $\beta_{33}=0.0133(5)$
$Fe^{+3}/Nb^{+5}/Ti^{4+}$	0.513(5)	0.0000	0.472(2)	$B=0.22(3)$	0.5000	0.5000	0.535(6)	$B=0.001(6)$
O_I^{-2}	0.51(1)	0.0000	−0.03(1)	$B=0.3(4)$	0.5000	0.5000	0.050(3)	$B=0.5(3)$
O_{II}^{-2}	0.279(5)	0.255(5)	0.427(5)	$B=0.2(3)$	0.5000	0.0000	0.571(2)	$B=0.3(2)$
	$R_p=7.79$, $R_{wp}=10.4$, $R_{exp}=8.39$, $\chi^2=1.53$				$R_p=9.57$, $R_{wp}=12.5$, $R_{exp}=9.97$, $\chi^2=1.56$			

selected compositions with $x=0.04$, 0.06, and 0.15, respectively, using the Cm, $Cm+P4mm$, and $P4mm$ space groups. In the inset of these figures we also show the Rietveld fits for a few selected pseudocubic reflections (200, 220, and 222). It is evident from Fig. 3 that the overall fit between the observed and calculated profiles is very good, with nearly flat difference profiles for all the three compositions. For $x=0.15$, the majority phase is although tetragonal but a very small amount of the monoclinic phase had to be taken into consideration to obtain good Rietveld fits. For $x=0.06$, we considered the orthorhombic $Cmm2$ space group also, as $Cmm2$ is a subgroup of $P4mm$ and a supergroup of Cm. But it not only gave a very poor fit but also could not account for all the reflections. This is illustrated for 200, 220, and 222 peaks with arrows in the inset of Fig. 3(b). In the absence of such an orthorhombic $Cmm2$ phase, the coexistence of tetragonal and monoclinic phases in the MPB region implies first order nature of MPB. Such a coexistence is well known in the MPB systems [PZT (Ref. 17) and PMN–xPT (Refs. 2 and 18)] also.

In view of the large anisotropic broadening of the monoclinic peaks in contrast to sharp tetragonal peaks, the phase fraction could not be obtained reliably from the integrated intensities. Phase fractions were therefore estimated using peak intensities obtained from the calculated Rietveld profiles. The variation in lattice parameters and the phase fraction of the monoclinic and tetragonal phases, obtained from the Rietveld refinements, are shown in Figs. 4(a) and 4(b), respectively. The refined parameters for pure monoclinic ($x=0.04$) and the nearly pure tetragonal ($x=0.15$) phases are listed in Table I. The equivalent perovskite cell parameters of the monoclinic phase a_p ($\sim a_m/\sqrt{2}$), b_p ($\sim b_m/\sqrt{2}$), and c_p ($\sim c_m$) are found to be 4.0124, 4.0087, and 4.0138 Å, respectively, for $x=0.04$. These values suggest that the monoclinic phase is of M_A type ($a_p \approx b_p < c_p$) in the sense of Vanderbilt and Cohen.[19] This M_A phase is similar to that reported in PZT (Refs. 1 and 17) but different from those reported in PMN–xPT which are of M_B and M_c types.[2,18]

Correlating our structural results with the composition dependent dielectric permittivity, we conclude that the peak in the room temperature dielectric permittivity in Fig. 1(b) is linked to a monoclinic to tetragonal morphotropic phase transition similar to that reported in PZT ceramics at the MPB.[10,17,20] The MPB region in PFN–xPT contains coexisting monoclinic and tetragonal phases over a finite compositional width (Δx). The dominant phase in the coexistence region is monoclinic for $x \leq 0.07$ [see Fig. 4(b)]. For $x \geq 0.08$, the dominant phase is tetragonal [Fig. 4(b)]. It is interesting to note that the peak value of the room temperature intrinsic dielectric permittivity at $x=0.08$ [Fig. 1(b)] corresponds to the onset of two phase region with dominant tetragonal phase content.

Satendra Pal Singh acknowledges AICTE and CSIR for partial financial support. The experiments at Pohang Light Source (PLS) were supported by the Korean Ministry of Science and Technology (MOST) and POSTECH, Pohang, Korea.

[1] B. Noheda, J. A. Gonzalo, L. E. Cross, R. Guo, S.-E. Park, D. E. Cox, and G. Shirane, Phys. Rev. B **61**, 8687 (2000).
[2] A. K. Singh and D. Pandey, Phys. Rev. B **67**, 064102 (2003).
[3] D. M. Hatch, H. T. Stokes, R. Ranjan, Ragini, S. K. Mishra, D. Pandey, and B. J. Kennedy, Phys. Rev. B **65**, 212101 (2002).
[4] D. Pandey, A. K. Singh, and S. Baik, Acta Crystallogr., Sect. A: Found. Crystallogr. **64**, 192 (2008).
[5] K. Ohwada, K. Hirota, P. W. Rehrig, Y. Fujii, and G. Shirane, Phys. Rev. B **67**, 094111 (2003).
[6] R. Haumont, A. Al-Barakaty, B. Dkhil, J. M. Kiat, and L. Bellaiche, Phys. Rev. B **71**, 104106 (2005).
[7] D. Berlincourt, Sandia Corporation Technical Report No. SC-4443(RR), 1960.
[8] B. Jaffe, W. R. Cook, and H. Jaffe, *Piezoelectric Ceramics* (Academic, London, 1971).
[9] S. Bhattacharjee, S. Tripathi, and D. Pandey, Appl. Phys. Lett. **91**, 042903 (2007).
[10] B. Noheda, D. E. Cox, G. Shirane, J. A. Gonzalo, L. E. Cross, and S.-E. Park, Appl. Phys. Lett. **74**, 2059 (1999).
[11] S. P. Singh, A. K. Singh, D. Pandey, H. Sharma, and O. Parkash, J. Mater. Res. **18**, 2677 (2003).
[12] J. Rodriguez-Carvajal, FULLPROF, May 2006, Laboratory Leon Brillouin (CEA-CNRS) CEA/Saclay, 91191 Gif sur Yvette Cedex, France.
[13] N. Lampis, P. Sciau, and A. G. Lehmann, J. Phys.: Condens. Matter **11**, 3489 (1999).
[14] A. K. Jonscher, *Dielectric Relaxation in Solids* (Chelsea, London, 1983).
[15] S. P. Singh, D. Pandey, S. Yoon, S. Baik, and N. Shin, Appl. Phys. Lett. **90**, 242915 (2007).
[16] S. P. Singh, A. K. Singh, and D. Pandey, J. Phys.: Condens. Matter **19**, 036217 (2007).
[17] A. K. Singh, S. K. Mishra, Ragini, D. Pandey, S. Yoon, S. Baik, and N. Shin, Appl. Phys. Lett. **91**, 192904 (2007).
[18] A. K. Singh, D. Pandey, and O. Zaharko, Phys. Rev. B **74**, 024101 (2006).
[19] D. Vanderbilt and M. H. Cohen, Phys. Rev. B **63**, 094108 (2001).
[20] Ragini, R. Ranjan, S. K. Mishra, and D. Pandey, J. Appl. Phys. **92**, 3266 (2002).